Interaction of plasma membrane fibronectin receptor with talin—a transmembrane linkage

Alan Horwitz*, Kimberly Duggan*, Clayton Buck†, Mary C. Beckerle‡ & Keith Burridge‡

* Department of Biochemistry and Biophysics, University of Pennsylvania School of Medicine, Philadelphia, Pennsylvania 19104, USA
† The Wistar Institute of Anatomy and Biology, 36th and Spruce Street, Philadelphia, Pennsylvania 19104, USA
‡ Laboratories for Cell Biology, Department of Anatomy, University of North Carolina School of Medicine, Chapel Hill, North Carolina 27514, USA

Many observations suggest the presence of transmembrane linkages between the cytoskeleton and the extracellular matrix. In fibroblasts both light and electron microscopic observations reveal a co-alignment between actin filaments at the cell surface and extracellular fibronectin[1–3]. These associations are seen at sites of cell matrix interaction, frequently along stress fibres and sometimes where these bundles of microfilaments terminate at adhesion plaques (focal contacts). Non-morphological evidence also indicates a functional linkage between the cytoskeleton and extracellular matrix. Addition of fibronectin to transformed cells induces flattening of the cells and a reorganization of the actin cytoskeleton, with the concomitant appearance of arrays of stress fibres[4–6]. Conversely, disruption of the actin cytoskeleton by treatment with cytochalasin B leads to release of fibronectin from the cell surface[7]. As yet, there is no detailed knowledge of the molecules involved in this transmembrane linkage, although several proteins have been suggested as candidates in the chain of attachment between bundles of actin filaments and the cytoplasmic face of the plasma membrane: these include vinculin[8], α-actinin[9] and talin[10], each one having been identified at regions where bundles of actin filaments interact with the plasma membrane and underlying cell-surface fibronectin[10–13]. Recently, the cell–substrate attachment (CSAT) antigen[14] has been identified as a plasma membrane receptor for fibronectin[15], raising the possibility that this glycoprotein complex may serve as a bridge between fibronectin and one or more of the underlying cytoskeletal components mentioned. Here we have investigated the interaction of the purified CSAT antigen with these cytoskeletal components, and we demonstrate an interaction specifically between the CSAT antigen and talin.

The CSAT antigen is an integral membrane glycoprotein complex recognized by the CSAT monoclonal antibody[16]. This antibody inhibits the adhesion and perturbs the morphology of several different avian cell types including fibroblasts, muscle cells and neurones[17,18]. The antigen consists of three distinct glycoproteins of relative molecular mass (M_r) ~140,000 (140K) on SDS gels[16]. The antigen co-localizes extensively with fibronectin along portions of stress fibres and is found at their termini[19]. Similar observations have been made using another monoclonal antibody, JG-22, directed against the same antigen[20–22]. Recently, the purified antigen has been shown to bind to fibronectin in a physiologically significant manner[15], being inhibited from binding by the fibronectin tetrapeptide (RGDS) that inhibits adhesion of cells to fibronectin[23]. Glycoproteins of M_r ~ 140K have also been implicated in the adhesion of mammalian cells to fibronectin[24,25]. This identification of the CSAT antigen as a fibronectin receptor has prompted further studies to determine whether it may also function as a link between fibronectin and cytoskeletal components.

Interaction between the CSAT antigen and vinculin, talin or α-actinin was assayed initially using Western blotting. The CSAT antigen was radio-iodinated and used to overlay nitrocellulose strips onto which these other proteins had been electrophoretically transferred from SDS gels. No significant binding was detected in this or in the reciprocal experiment, when vinculin, talin and α-actinin were used as radiolabelled probes. Similarly, no binding was observed in sedimentation experiments in which the CSAT antigen was mixed individually with the proteins prior to sucrose density gradient centrifugation. The lack of detectable binding in the latter assay might have been caused by rapid dissociation of receptor–ligand complexes, therefore we used the technique of equilibrium gel filtration: in this method a gel filtration column is pre-equilibrated with the ligand to be assayed (talin, vinculin or α-actinin). The ligands and CSAT antigen (labelled with ^{35}S-methionine) were then incubated for 30 min before loading onto the column. (Further details of the assay are presented elsewhere[15].) The method ensures receptor occupancy for rapidly dissociating receptor–ligand complexes.

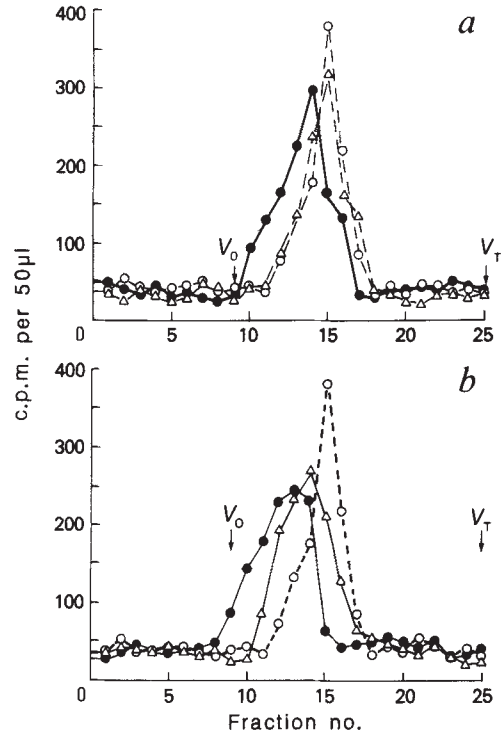

Fig. 1 *a*, Profile of elution of CSAT antigen from gel-filtration columns pre-equilibrated with talin. The CSAT antigen was passed through a column equilibrated with 900 μg ml^{-1} vinculin (△) or 500 μg ml^{-1} talin (●). ○, CSAT antigen alone. *b*, Profile of elution of CSAT antigen from gel-filtration columns pre-loaded with: 800 μg ml^{-1} fibronectin and 200 μg ml^{-1} talin (●) or 800 μg ml^{-1} fibronectin, 200 μg ml^{-1} talin and 1 mg ml^{-1} of the cell-binding tetrapeptide (RGDS) from fibronectin (Peninsula Laboratories, Belmont, California) (△). ○, CSAT antigen alone.
Methods. Gel filtration was performed using Ultrogel AcA22 (LKB) in a column of 0.2 × 30 cm bed volume. The column was first pre-loaded with the appropriate ligand in buffer B (20 mM NaCl, 20 mM Tris, 0.1 mM EDTA, 0.1 mM EGTA, 0.1% β-mercaptoethanol, 0.1% Nonidet P-40 (NP40), *p*H 7.6). Similar results were obtained using TNC buffer (0.01 M Tris–acetic acid, 0.5 mM $CaCl_2$, 0.15 M NaCl, 0.1% NP40, *p*H 8.0). The ligands and CSAT antigen (2.2×10^5 mCi mmol^{-1}) were incubated for 30 min before loading onto the ligand-pre-equilibrated column[15]. Fractions (60 μl) were collected and 50 μl of each fraction were counted; V_0 and V_T, void and included volumes, respectively. The CSAT antigen was purified from ^{35}S-methionine-labelled chicken tendon fibroblasts using immunoaffinity chromatography with the CSAT monoclonal antibody as the immunoabsorbent[15,16]. The cytoskeletal proteins talin, vinculin and α-actinin used in this and the other experiments were purified from chicken gizzard smooth muscle essentially as described previously[10,30].

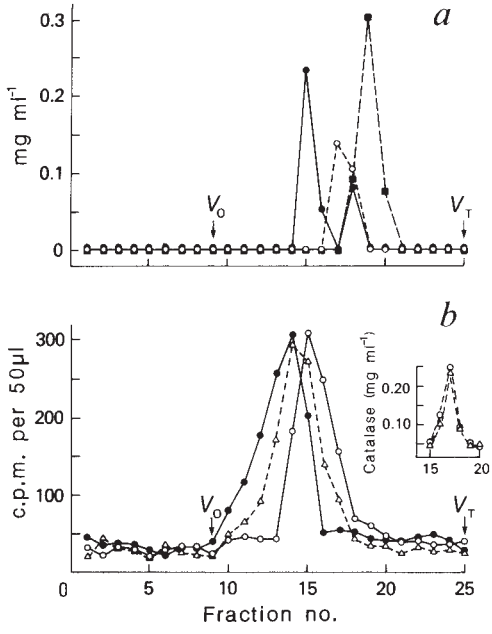

Fig. 2 *a*, Gel-filtration elution profiles (mg ml^{-1}) of talin (○), vinculin (■), and talin–vinculin complex (●), using Ultrogel AcA22. Equal amounts of talin and vinculin were incubated together on ice for 2 h, brought to room temperature, then analysed by gel filtration. Protein concentrations were determined by the method of Lowry *et al.*[31]. *b*, Profile of elution of the CSAT antigen from gel-filtration columns pre-equilibrated with 200 μg ml^{-1} talin (△), 200 μg ml^{-1} vinculin (○), or 200 μg ml^{-1} talin plus 200 μg ml^{-1} vinculin (●). Inset, the elution positions (mg ml^{-1}) of a catalase (20 μg) Stokes radius standard when added to either the CSAT antigen–talin mixture (△) or the CSAT antigen–vinculin mixture (○) before gel filtration. Protein concentrations were determined by the method of Lowry *et al.*[31], and the background values due to ligand subtracted. Gel filtration was performed as described in Fig. 1 legend.

Figure 1*a* shows the elution profile of the detergent-solubilized CSAT antigen during gel filtration on Ultrogel AcA22 (LKB). The antigen is seen as a single peak eluting between fractions 13 and 18. When the column was first pre-loaded with talin at concentrations >25 μg ml^{-1}, the elution profile shifted towards a higher effective Stokes radius, revealing an interaction between the CSAT antigen and talin. Such shifts were not seen when the mixtures of the CSAT antigen and talin were added to a column that had not been pre-loaded with talin, indicating that the complex formed between the two proteins tends to dissociate rapidly on the timescale of the molecular sieving. The magnitude of the shift increased with increasing talin concentration, reaching a plateau at ~300 μg ml^{-1}. The half-maximal shift was at ~150 μg ml^{-1}, which corresponds to a dissociation constant, K_d, of $\sim 7 \times 10^{-7}$ M. The elution profile of the antigen during gel filtration in a column pre-equilibrated with either 900 μg ml^{-1} vinculin (Fig. 1*a*) or 2 mg ml^{-1} α-actinin (not shown) was identical to those seen with columns that had not been pre-equilibrated with a ligand. The 'talin shift' was observed in each of 21 separate determinations using 3 different antigen and talin preparations. The elution profile of catalase, a Stokes radius standard, when added to the CSAT antigen–vinculin and CSAT antigen–talin mixtures prior to gel filtration, was invariant (see Fig. 2 inset), as reported previously for fibronectin and laminin[15].

The physiological significance of the interaction between the CSAT antigen and fibronectin was established[15] by its inhibition using the fibronectin cell-binding tetrapeptide. We have included this same tetrapeptide with talin during equilibrium gel filtration and observed no effect on the formation of the talin–CSAT antigen complex. This result indicates that talin and fibronectin bind to separate sites on the CSAT antigen; this has been confirmed in further experiments in which it was found that when both fibronectin and talin were present during gel filtration, there was a larger shift in the CSAT antigen elution profile than occurred in the presence of either ligand alone (Fig. 1*b*). Moreover, the presence of the fibronectin cell-binding tetrapeptide diminished the magnitude of this shift to one similar to that seen with talin alone (Fig. 1*b*).

It has been demonstrated previously that vinculin and talin form a complex of moderately high affinity[26]. This complex can also be seen by gel filtration (Fig. 2*a*): 80% of the total protein migrates in the complex at a higher effective Stokes radius. We have assayed the interactions of the complex with the purified CSAT antigen. Pre-loading of the gel filtration column with the talin–vinculin complex also shifted the elution profile of the antigen (Fig. 2*b*); but the magnitude of this shift was consistently larger than that observed with talin alone. The simultaneous interaction of talin with both the CSAT antigen and vinculin indicates that talin has separate binding sites for the two molecules.

It has been shown that talin is highly susceptible to proteolysis, resulting in the cleavage of the molecule into two domains of M_r ~190K and 46K (refs 27, 28). In some systems, such as platelet activation, this proteolysis appears to be physiologically significant and involves a calcium-dependent protease[27,28]. Previous work has shown that the larger talin domain binds vinculin[29], and we queried whether proteolysis would separate the vinculin-binding domain from the CSAT antigen-binding domain. When the purified 190K fragment of talin was substituted for talin in the equilibrium gel filtration assays, however, it behaved like intact talin and induced an indistinguishable shift in the elution profile of the CSAT antigen (data not shown), indicating that this large talin domain contains binding sites for both vinculin and the CSAT antigen.

The transmembrane link between fibronectin and the actin cytoskeleton has been elusive. Several observations have implicated the CSAT antigen as a component in this linkage: (1) the CSAT monoclonal antibody inhibits adhesion and perturbs the morphology of several different cell types[14,17,18], (2) the antigen is localized in regions of cell adhesion and putative transmembrane coupling[19], (3) the antigen appears to span the membrane, as suggested by the existence of two classes of monoclonal antibodies that bind to either intact or saponin-permeabilized cells (C.B., C. Decker and A.H., unpublished observations), (4) the antigen is an oligomeric complex of three integral membrane glycoproteins which serves as a cell-surface receptor for fibronectin and other extracellular matrix molecules[15,16]. We have now shown that the CSAT antigen has a binding domain for talin, a protein associated with the actin cytoskeleton. Although talin has been shown to bind vinculin, it remains to be established how talin or the talin–vinculin complex interacts with actin. We conclude that the CSAT antigen appears to function in transmembrane linkage as a dual receptor possessing at least two distinct classes of binding domains: one for extracellular molecules like fibronectin and the other for cytoskeletal proteins such as talin.

This work was supported by NIH grants GM 23244 (to A.H.), CA 19144 and 10815 (to C.B.) and GM 29860 (to. K.B.), and by the H. M. Watts Jr Neuromuscular Disease Research Center (A.H.).

Received 21 January; accepted 7 February 1986.

1. Hynes, R. O. & Destree, A. T. *Cell* **15**, 875–886 (1978).
2. Heggeness, M. H., Ash, J. F. & Singer, S. J. *Ann. N.Y. Acad. Sci.* **312**, 414–417 (1978).
3. Singer, I. I. *Cell* **16**, 675–685 (1979).
4. Yamada, K. M., Ohanian, S. H. & Pastan, I. *Cell* **9**, 241–245 (1976).
5. Ali, I. U., Mautner, V., Lanza, R. & Hynes, R. O. *Cell* **11**, 115–126 (1977).
6. Willingham, M. C., Yamada, K. M., Yamada, S. S., Pouyssegur, J. & Pastan, I. *Cell* **10**, 375–280 (1977).
7. Ali, I. U. & Hynes, R. O. *Biochim. biophys. Acta* **471**, 16–24 (1977).
8. Geiger, B. *Cell* **18**, 193–205 (1979).

9. Lazarides, E. & Burridge, K. *Cell* **6**, 289-298 (1975).
10. Burridge, K. & Connell, L. *J. Cell Biol.* **97**, 359-367 (1983).
11. Burridge, K. & Feramisco, J. R. *Cell* **19**, 587-595 (1980).
12. Singer, I. I. & Paradiso, P. R. *Cell* **24**, 481-492 (1981).
13. Chen, W. T. & Singer, S. J. *J. Cell Biol.* **95**, 205-233 (1982).
14. Neff, N. T. *et al. J. Cell Biol.* **95**, 654-666 (1982).
15. Horwitz, A., Duggan, K., Greggs, R., Decker, C. & Buck, C. *J. Cell Biol.* **101**, 2134-2144 (1985).
16. Knudsen, K., Horwitz, A. & Buck, C. *Expl Cell Res.* **157**, 218-226 (1985).
17. Decker, C., Greggs, R., Duggan, K., Stubbs, J. & Horwitz, A. *J. Cell Biol.* **99**, 1398-1404 (1984).
18. Bozyczko, D. & Horwiz, A. *J. Neurosci.* (in the press).
19. Damsky, C., Knudsen, K., Bradley, D., Buck, C. & Horwitz, A. *J. Cell Biol.* **100**, 1528-1539 (1985).
20. Greve, J. M. & Gottlieb, D. I. *J. cell. Biochem.* **18**, 221-230 (1982).
21. Chen, W. T., Hasegawa, E., Hasegawa, T., Weinstock, C. & Yamada, K. M. *J. Cell Biol.* **100**, 1103-1114 (1985).
22. Hasegawa, T., Hasegawa, E., Chen, W. T. & Yamada, K. M. *J. cell. Biochem.* **28**, 307-318 (1985).
23. Pierschbacher, M. & Ruoslahti, E. *Nature* **309**, 30-33 (1984).
24. Brown, P. J. & Juliano, R. *Science* **228**, 1448-1451 (1985).
25. Pytela, R., Pierschbacher, M. & Ruoslahti, E. *Cell* **40**, 191-198 (1985).
26. Burridge, K. & Mangeat, P. H. *Nature* **308**, 744-745 (1984).
27. O'Halloran, T. O., Beckerele, M. C. & Burridge, K. *Nature* **317**, 449-451 (1985).
28. Beckerele, M. C., O'Halloran, T. O. & Burridge, K. *J. cell. Biochem.* (in the press).
29. O'Halloran, T. O. & Burridge, K. *Biochim. biophys. Acta* (in the press).
30. Feramisco, J. R. & Burridge, K. *J. biol. Chem.* **255**, 1194-1199 (1980).
31. Lowry, O. H., Rosebrough, N. J., Farr, A. L. & Randall, R. J. *J. biol. Chem.* **193**, 265-275 (1951).

Envelope structure of Semliki Forest virus reconstructed from cryo-electron micrographs

R. H. Vogel, S. W. Provencher*, C.-H. von Bonsdorff†, M. Adrian & J. Dubochet

European Molecular Biology Laboratory, Postfach 102209, D-6900 Heidelberg, FRG

The basic principles of the architecture of many viral protein shells have been successfully established from electron microscopy and X-ray data[1-4], but enveloped viruses have been more difficult to study because they resist crystallization and are easily deformed when prepared for electron microscopy. To avoid the limitations of conventional techniques when applied to enveloped viruses, we have used a cryo-electron microscopy method in which unfixed and unstained viruses are observed in an unsupported thin layer of vitrified suspension[5,6]. Because of electron beam damage, the many different views required for high-resolution three-dimensional reconstruction cannot be obtained from a tilt series of the same particle. The images of many differently oriented viruses are combined using a novel reconstruction method, 'reconstruction by optimized series expansion' (ROSE)[7]. The structure of the envelope of Semliki Forest virus has been reconstructed to 3.5-nm resolution. The $T = 4$ geometry of the surface lattice, the shape of the trimeric spikes and their arrangement on the lipid bilayer are visualized.

Semliki Forest virus (SFV) is one of the simplest icosahedral enveloped RNA viruses[8-11]. The centre of the virus consists of the nucleocapsid, surrounded by the lipid bilayer at an average radius of 23 nm. The spike proteins protruding from the lipid bilayer are each formed by three polypeptide chains with a total relative molecular mass of 100,000. They extend to an outer radius of ~32 nm.

Figure 1 shows a focus series of SFV in a thin layer of vitrified buffer solution. The visualized aspects of the virus depend strongly on the focus. This is because, unlike in conventionally stained specimens, the contrast is essentially due to phase contrast[12]. The focus values of the four micrographs in the series have been chosen to give an optimal coverage of the information contained in the specimen. Coarse features such as the triangulation number $T = 4$ of the icosahedral shell are best observed in strongly underfocused images (Fig. 1*d*; see also refs 5, 6). Fine details, such as the lipid bilayer, are visible close to focus (Fig. 1*a*, arrows).

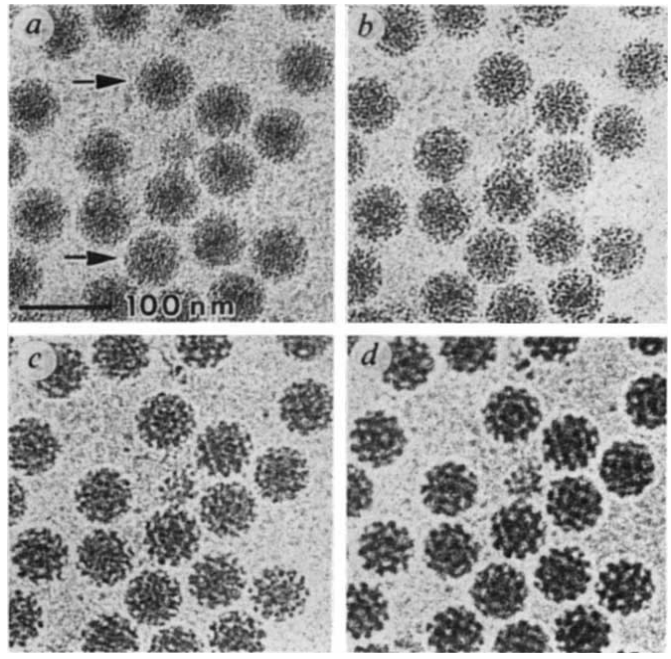

Fig. 1 Focus series of a thin vitrified unsupported layer of unfixed and unstained Semliki Forest virus suspension. The specimen has been prepared by the perforated grid method[5]: a drop of suspension was applied to a copper grid supporting a perforated carbon film. Most of the drop was removed with blotting paper and the grid was immediately immersed in undercooled liquid ethane. The grid, always kept below −160 °C, was transferred and observed in a Philips 400 electron microscope working at 80 kV and equipped with the cold stage PW6591/100. The micrographs were recorded at an electron magnification of ×33,000 and the electron dose was 1,000 electrons per nm^2 per micrograph. Micrographs *a*–*d* are underfocused by 1.5, 3, 6 and 11 μm respectively. These values have been chosen so that the first zero of the transfer function of one micrograph corresponds to the first maximum of the preceding one (see ref. 6, Fig. 5, for illustration). The first maximum corresponds to 3.5 nm in *a* and to 9.5 nm in *d*. In these conditions the four micrographs together retrieve at least 70% of the information in the spatial frequency band corresponding to 3–12 nm. The arrows in *a* point towards particles where the lipid bilayer is visible.

Using the series shown in Fig. 1, a three-dimensional reconstruction of the virus has been obtained with ROSE[7] (S.W.P. and R.H.V., manuscript in preparation). Various representations of the reconstruction at different resolution are shown in Figs 2–4. The surface of the virus, consisting of 80 spikes, is arranged in a $T = 4$ surface lattice. The concept of quasi-equivalence[1] applied to this geometry requires that each spike be a trimer of spike proteins (that is, 3×3 polypeptide chains). The reconstruction shows that the spikes are indeed triangular. The total number of spike proteins should therefore be 240. This implies that the total mass of the virus should be higher than the value obtained by several direct mass measurement methods[13,14]. As can be seen from the reconstruction, the suggestion that the virus has a triangulation number $T = 3$ for resolving the discrepancy is ruled out. Another more subtle geometrical prediction is that peripentonal spikes must have a different conformation from those of the 3-fold axes[15]. This prediction is supported by the reconstruction in that the peripentonal spikes have a concave surface whereas those centred on the 3-fold axes are convex (Fig. 2).

* Permanent address: Max-Planck-Institut für biophysikalische Chemie, Postfach 2841, D-3400 Göttingen, FRG.
† Present address: Department of Virology, University of Helsinki, SF-00290 Helsinki 29, Finland.